Eur. Phys. J. A **18**, 65–73 (2003)
DOI 10.1140/epja/i2002-10168-7

THE EUROPEAN PHYSICAL JOURNAL A

Cluster structure of ^{16}O

M.N.A. Abdullah[1], S. Hossain[1,2], M.S.I. Sarker[1], S.K. Das[1,2], A.S.B. Tariq[1], M.A. Uddin[1], A.K. Basak[1,a], S. Ali[3], H.M. Sen Gupta[3], and F.B. Malik[4]

[1] Department of Physics, University of Rajshahi, Rajshahi, Bangladesh
[2] Department of Physics, Shahjalal University of Science & Technology, Sylhet, Bangladesh
[3] Department of Physics, University of Dhaka, Dhaka, Bangladesh
[4] Department of Physics, Southern Illinois University, Carbondale, Illinois 62901, USA

Received: 5 December 2002 /
Published online: 9 October 2003 – © Società Italiana di Fisica / Springer-Verlag 2003
Communicated by A. Molinari

Abstract. A folding potential describing the α-scattering on ^{16}O over a broad energy range 25.8–146.0 MeV is constructed on the basis of α-like cluster and unclustered-nucleon configurations of ^{16}O. The resulting potential does not need any renormalization to fit the angular distribution of elastic cross-sections. The effects of the repulsive part of α-α and α-nucleon interactions are investigated. The analysis suggests that both the α-α repulsive potential and the unclustered nucleonic configuration in the target are important to describe the scattering data over a broad range of incident energies. The root-mean-square radius for the ^{16}O nucleus is deduced.

PACS. 25.55.Ci Elastic and inelastic scattering – 24.10.Ht Optical and diffraction models – 21.60.Gx Cluster models

1 Introduction

According to the resonating group model [1], the nucleons in a nucleus cluster together in all possible ways with varying probabilities. The clusters are continually broken up and reformed in a new way. The total wave function may be expressed in terms of a series of the cluster wave functions with appropriate coefficients. Of course, the α-like cluster is the most likely as it has by far the highest binding energy and is compact enough to fit in the inter-nucleon distance in a nucleus [2].

The elastic scattering of α-particles of a few tens of MeV has been analyzed using the single-folding [3–8] and the double-folding [9–16] models. The results of these analyses show that a renormalization factor $N_r = 1.19$–1.39 is required for the folded potential. The single-folding calculations of Yong-Xu and Qing-Run [3,4] based on the α-cluster model for the α+^{16}O system give the renormalization factors around $N_r = 0.84$ which is less than unity. In the work on the α-elastic scattering on ^{12}C and ^{16}O, Khallaf *et al.* [16] have managed to obtain N_r =1 by introducing additional parameters, β_R and β_I (for a complex folded potential), which in effect, normalize the potential. However, the model seems unsatisfactory for incident energies less than 52 MeV and, as a consequence, the analysis omits data in the energy range of 25.4–48.8 MeV, where back angle data are available. An intriguing aspect of obtaining remarkable fits to the elastic data in the previous works [6,10,13,14] is the use of energy-dependent renormalization factors.

Of the two recent papers using folding model potentials to fit α-elastic scattering data on ^{16}O, Farid *et al.* [6] have analyzed the data in the energy range 32.2–146 MeV employing two alternative single-folded potentials, one over α-cluster density distribution and the other over nucleonic density using an energy-dependent normalization factor N_r. They left out the elastic-scattering data for the energies 39.3, 49.5, 69.5 MeV and energies below 32.2 MeV. In another paper, Khoa [15] has analyzed the angular distributions of cross-section for three incident energies *viz.* 54.1, 80.7 and 104 MeV, where data are limited to only about 100° scattering angles for the two latter energies.

Data of the α-^{16}O elastic scattering are available in the literature [10,12,17–20] over a broad spectrum of incident energies. We shall primarily concentrate on elastic-scattering data with wide angular distributions. Our aim is to describe the α-^{16}O elastic-scattering data from 25.4 to 146.0 MeV by a single-folding model, which can generate α-nucleus potentials that do not need renormalization at different incident energies. To this end, we take the view that most of the time, a number of nucleons are primarily in α-like clusters and the rest are in an unclustered configuration. Thus, in this picture the wave function of a

[a] e-mail: akbasak-phy@ru.ac.bd

nucleus can be considered as the product of wave functions of α-like configurations and those of unclustered nucleonic configurations. This, as shown below, leads to a sum of two folding potentials, one convoluted over α-density distribution and another over nucleonic density distribution.

In the following section we present a theoretical framework for the proposed model, based on a composite distribution of α-like clusters and unclustered nucleons in the target nucleus, to work out an appropriate folded potential. The analysis is given in sect. 3. Section 4 deals with the discussion and conclusions.

2 Formalism

Following the work of [21] and noting that the composite system of an incident α-particle and a target nucleus having A nucleons is in a meta-stable state, its wave function Ψ at a given time may be expanded in an orthonormal set Φ_n as

$$\Psi(1,\ldots,A+4)=\sum_n A_n\Phi_n(1,\ldots,A+4). \tag{1}$$

The numbers in parentheses refer to coordinates. The amplitude $A_n=(\Phi_n,\Psi)$ determines the amount of a particular configuration present in the composite system at a given time. The integration is over all coordinates. In this case, Ψ is normalized to $(A+4)$, *e.g.*

$$\sum_n |A_n|^2=(A+4). \tag{2}$$

In the model space of target-projectile, both Φ_n and the total Hamiltonian H may be expressed in terms of relative coordinate $\mathbf{R}$ of the alpha-target system and the intrinsic coordinates of nucleons in incident alpha and target nuclei marked as primes with anti-symmetrization:

$$\begin{aligned}\Phi_n=&\sum_{i\beta} f_{ni\beta}(\mathbf{R})\,\psi_{ni}(1',\ldots,A')\\ &\times\phi_{n\beta}\big((A+1)',\ldots,(A+4)'\big)\end{aligned} \tag{3}$$

and

$$\begin{aligned}H=&-\frac{\hbar^2}{2M}\nabla_R^2+H_0(1',\ldots,A')\\ &+H_\alpha\big((A+1)',\ldots,(A+4)'\big)\\ &+H_{\rm int}\big(\mathbf{R},1',\ldots,(A+4)'\big).\end{aligned} \tag{4}$$

Here M is the reduced mass. $H_{\rm int}$ represents the potential between the nucleons in the incident α-particle and the nucleons in the target nucleus. Because of the orthonormality condition, one gets the following equation:

$$\begin{aligned}&\left[-\frac{\hbar^2}{2M}(\nabla_R^2+k_{ni\beta}^2)+V_{nnii\beta\beta}(\mathbf{R})+K_{nnii\beta\beta}(\mathbf{R})\right]f_{ni\beta}(\mathbf{R})\\ &\quad=\sum\left[V_{mnij\beta\mu}(\mathbf{R})+K_{mnij\beta\mu}(\mathbf{R})\right]f_{mi\mu}(\mathbf{R}).\end{aligned} \tag{5}$$

In eq. (5) the summation on the right side runs over all cases other than $m=n$, $i=j$ and $\mu=\beta$. The potential $V_{mnij\beta\mu}$ is given by

$$V_{mnij\beta\mu}(\mathbf{R})=(\psi_{ni}\varphi_{n\beta},H_{\rm int}\psi_{mj}\varphi_{m\mu}). \tag{6}$$

ψ_{ni} and $\varphi_{n\beta}$ are, respectively, the wave functions of H_0 and H_α with eigenvalues E_{ni} and $E_{n\beta}$ satisfying $\hbar^2k_{ni\beta}^2/2M=E-E_{ni}-E_{n\beta}$.

$K_{mnij\beta\mu}$, in (5), is the non-local potential originating from the Pauli principle. If the projectile α is considered as a boson in isolation, the exchange contributions between the incident α and α-like as well as single-fermion–like configurations in the target nucleus may be neglected in the first approximation. Furthermore, in the absence of sharp resonances, the energy-averaged contribution of the coupling terms leads to a complex potential [22–24]. Thus, the net effect of these coupling terms is to add an imaginary term to the diagonal part of the interaction potential. In this approximation, by dropping the subscripts and denoting the average potential between the projectile α and the target due to $H_{\rm int}$ by $U(R)$, eq. (5) can be cast to the simple form

$$\left[-\frac{\hbar^2}{2M}\left(\nabla^2+k^2\right)+U(R)\right]f(\mathbf{R})=0. \tag{7}$$

Following eq. (6), one can write

$$U(R)=V_{nniiββ}=(\psi_{ni}\varphi_{n\beta},H_{\rm int}\psi_{ni}\varphi_{n\beta}). \tag{8}$$

We assume that $(1,2,\ldots,x)$ nucleons are in cluster-like state and $((x+1),\ldots,A)$ in unclustered nucleonic state in the target. Denoting the c.m. coordinate of the α-projectile by $\mathbf{R}_\alpha$ and the coordinates of the nucleons in α-like cluster and unclustered nucleons as indexed by i and j, respectively, one can write (8) in the following approximate form:

$$\begin{aligned}U(R)=\Bigg(&\psi_{ni}\varphi_{n\beta}(\mathbf{R}_\alpha),\Big[\sum_{i=1}^{x}H_{\rm int}(\mathbf{R},|\mathbf{r}_i-\mathbf{R}_\alpha|)\\ &+\sum_{j=x+1}^{A}H_{\rm int}(\mathbf{R},|\mathbf{r}_j-\mathbf{R}_\alpha|)\Big]\psi_{ni}\varphi_{n\beta}(\mathbf{R}_\alpha)\Bigg).\end{aligned} \tag{9}$$

Approximating the target function by

$$\psi_{ni}(1',\ldots,A')\approx\phi_\alpha(1',\ldots,x')\,\phi_N((x+1)',\ldots,A') \tag{10}$$

with ϕ_α and ϕ_N as the part functions for the α-like and unclustered nucleonic configurations, respectively, and integrating over $\mathbf{R}_\alpha$, one can write eq. (9) in the form

$$\begin{aligned}U(R)=\Bigg(&\phi_\alpha(1',\ldots,x')\,\phi_N\big((1+x)',\ldots,A'\big),\\ &\Big[\sum_{i=1}^{x}V_{\alpha\alpha}(|\mathbf{R}-\mathbf{r}_i|)+\sum_{j=x+1}^{A}V_{\alpha N}(|\mathbf{R}-\mathbf{r}_j|)\Big]\\ &\times\phi_\alpha(1',\ldots,x')\,\phi_N\big((1+x)',\ldots,A'\big)\Bigg).\end{aligned} \tag{11}$$

Here $V_{\alpha\alpha}$ and $V_{\alpha N}$ denote, respectively, the interaction potentials of the projectile with the α-like clusters and unclustered nucleons in the target.

If one denotes the density-distributions of the α-like clusters and unclustered nucleons in the target by ρ_α and ρ_N, respectively, one can write eq. (11) in the form

$$U(R) = \int \rho_\alpha(\mathbf{r}_\alpha)\, V_{\alpha\alpha}(|\mathbf{R}-\mathbf{r}_\alpha|)\, \mathrm{d}^3\mathbf{r}_\alpha + \int \rho_N(\mathbf{r}_N)\, V_{\alpha N}(|\mathbf{R}-\mathbf{r}_N|)\, \mathrm{d}^3\mathbf{r}_N. \quad (12)$$

We note that, although the Buck potential [25] has customarily been used, this potential is determined from the low-energy α-α scattering data and not from the data at the energies considered herein. Similarly, Ali-Bodmer ℓ-dependent potential [26] deals with the α-scattering data up to about 23 MeV, which is well below the energy range studied herein. Adopting the basic premise of Ali and Bodmer that the non-locality in the α-α potential effectively introduces a short-range repulsion, we add such a part to the Buck potential at shorter range but keeping the latter potential intact at the longer range. For the α-N interaction potential, we take the simple Gaussian form, suggested in the review article of Ali *et al.* [27] on the basis of the work of Sack *et al.* [28]. Sack *et al.* obtained the parameters of the interaction from the fits to the $p_{\frac{1}{2}}$ and $p_{\frac{3}{2}}$ phase-shifts up to $E_p = 10$ MeV (lab). This corresponds to the maximum α-energy of 40 MeV (lab), which is again well below the higher energies considered herein. The repulsive potential noted above is expected to take care of the data at higher energies.

Equation (12), which is used to generate our folded potential $U(R)$, comprises the following assumptions:
i) The target nucleons are considered to be in the α-like cluster configuration for most of the time and in the unclustered nucleonic configuration for the rest of the time with the coexistence of these two configurations.
ii) Although the α-like clusters are transient giving rise to continual changes of position coordinates of the clusters and the nucleons in the target, the folded potentials convoluted from their density distributions are constant in time.

The density functions are considered here to be of both the following two forms, as suggested by Buck *et al.* [29]: The first one has a modified Gaussian shape [6,29] given by

$$\rho_i(r) = \rho_{0i}^{\mathrm{G}}\left(1 + w_{\mathrm{G}} r^2\right)\exp\left(-\beta_i r^2\right) \text{ with } i = \alpha,\ N. \quad (13)$$

The second one is a 3-point Fermi distribution [30] given by

$$\rho_i(r) = \rho_{0i}^{\mathrm{F}}\left(1 + w_{\mathrm{F}}\frac{r^2}{c_i^2}\right)\left[1 + \exp\left(\tfrac{r-c_i}{a_i}\right)\right]^{-1} \text{ with } i = \alpha,\ N. \quad (14)$$

If one interprets that the nucleus is composed of $4A_\alpha$ nucleons making A_α α-like clusters and A_N unclustered nucleons, then one can write the normalization integral as

$$\int \rho_\alpha(\mathbf{r}_\alpha)\, \mathrm{d}^3\mathbf{r}_\alpha + \int \rho_N(\mathbf{r}_N)\, \mathrm{d}^3\mathbf{r}_N = 4A_\alpha + A_N = A_T. \quad (15)$$

If the values of the parameters in the density distributions $\rho_\alpha(\mathbf{r}_\alpha)$ and $\rho_N(\mathbf{r}_N)$ are such that the integral value A_T in (15) is different from the target mass number A, then one may define the renormalization factor N_r [3–16], which has been found to be energy dependent, as

$$A_T(E) = N_r(E)\, A. \quad (16)$$

Following the assumption of our model including the basic premise of [26], the α-α potential can be parametrized as

$$V_{\alpha\alpha}(r) = V_R \exp\left(-\mu_R^2 r^2\right) - V_A \exp\left(-\mu_A^2 r^2\right). \quad (17)$$

In eq. (17), V_R and V_A are the repulsive and attractive parts of the potential with the range parameters μ_R and μ_A, respectively. The ℓ-independence of the repulsive part is considered for the sake of simplicity of the potential.

For the α-N potential, the following form [27] has been used:

$$V_{\alpha N}(r) = -V_0 \exp\left(-K^2 r^2\right), \quad (18)$$

with K as the range parameter.

For the imaginary part of the α-nucleus potential the phenomenological Gaussian form,

$$W(R) = -W_0 \exp\left(-\frac{R^2}{R_W^2}\right), \quad (19)$$

has been assumed. The Coulomb potential V_{C} of a uniformly charged sphere with radius $R_{\mathrm{C}} = r_{\mathrm{C}} A^{1/3}$,

$$V_{\mathrm{C}}(r) = \left[\tfrac{Z_1 Z_2 e^2}{2R_{\mathrm{C}}}\right]\left[3 - \tfrac{r^2}{R_{\mathrm{C}}^2}\right] \text{ for } r \le R_{\mathrm{C}} \quad = \tfrac{Z_1 Z_2 e^2}{r} \text{ for } r > R_{\mathrm{C}}, \quad (20)$$

is added to obtain the total α-nucleus potential.

3 Analysis

Analyses have been carried out using the optical model code SCAT2 [31] coupled with the χ^2-minimization code MINUIT [32]. The code SCAT2 has been modified to accommodate the folding calculations. In the analyses, the parameter values $V_A = 122.62$ MeV and $\mu_A = 0.469\,\mathrm{fm}^{-1}$ in eq. (17), taken from Buck *et al.* [25], and $V_0 = 47.3$ MeV and $K = 0.435\,\mathrm{fm}^{-1}$ in eq. (18), taken from [28], have been kept fixed. The Coulomb radius parameter has been set to $r_{\mathrm{C}} = 1.35$ fm.

3.1 Analysis using the modified Gaussian distribution

In the first phase of the analysis, the modified Gaussian density (MGD) ditribution in (13) with the parameter values $w_{\mathrm{G}} = 0.467$ and $\beta_\alpha = \beta_N = 0.292$, taken from [29],

Table 1. Energy-dependent parameters for folding potential using only the attractive part of α-α potential in the first step of analysis with the modified Gaussian density distribution. E_α and W_0 are in MeV, $\rho^{\rm G}_{0\alpha}$, in fm^{-3}, and β_α, in fm^{-2}. $J_R/(4A)$ and $J_I/(4A)$ are in MeVfm^3.

	First step with Gaussian distribution						
E_α	$\rho^{\rm G}_{0\alpha}$	A_T	N_r	W_0	χ^2	$J_R/(4A)$	$J_I/(4A)$
25.4	0.0346	16.60	1.038	8.0	1296	392.2	28.8
26.6	0.0361	17.32	1.083	10.0	4368	409.2	35.9
30.0	0.0355	17.03	1.064	10.2	2307	402.4	36.7
32.2	0.0356	17.08	1.068	13.0	4245	404.5	46.7
39.3	0.0352	16.89	1.056	17.2	11957	399.0	61.8
40.4	0.0354	16.98	1.061	17.3	643	401.3	62.2
48.8	0.0359	17.22	1.076	18.5	19508	406.9	66.5
49.5	0.0359	17.22	1.076	22.0	1333	406.9	79.1
54.1	0.0358	17.18	1.074	24.0	1130	405.8	86.3
65.0	0.0320	17.35	0.959	30.5	1405	362.7	109.6
69.5	0.0345	16.56	1.035	30.6	437	391.1	110.0
80.7	0.0330	15.83	0.989	32.5	373	374.1	116.8
104.0	0.0305	14.63	0.914	33.5	898	345.7	120.4
146.0	0.0270	12.95	0.809	34.0	311	306.0	122.2

has been employed. $\rho^{\rm G}_{0\alpha}$ and $\rho^{\rm G}_{0N}$ are treated as free parameters with the constraint that the integral value of A_T in (15) remains close to the number of nucleons A in the target. To elucidate the importance of contributions from the α-N potential arising from the unclustered nucleons and from the repulsive part of the α-α interaction, the analyses have been performed in the following three steps:
i) In the first step, only the attractive part of the α-α interaction has been employed to calculate the folded α-nucleus potential.
ii) In the second step, the α-N potential has been added to the α-α attractive potential for the calculation of the folded potential.
iii) In the final stage, the full analysis has been made with the folded potential arising from the attractive and repulsive parts of the α-α interaction, and the α-N potentials.

In the first step of the analysis with the MGD distribution in (13), only the folding potential arising from the attractive part of the α-α interaction potential has been employed. Thus, $\rho^{\rm G}_{0N}$ has been set to zero, and $\rho^{\rm G}_{0\alpha}$ and the parameters W_0 and R_W of the imaginary part of the α-^{16}O potential in (19) have been adjusted to obtain the best possible fit to the data at each of the incident energies. The $R_W = 3.55$ fm value gives the best overall fit to the data at all the energies. Table 1 shows the values of $\rho^{\rm G}_{0\alpha}$, W_0, A_T and the renormalization factor N_r for the best fits to the data at the different incident energies. The volume integrals for the real and imaginary parts of the α-nucleus potential, $J_R/(4A)$ and $J_I/(4A)$, respectively, are also noted in table 1 for the different energies. The sum of the χ^2-values over all the incident energies is $\chi^2_T = 50211$. The calculated cross-sections are compared to the data in fig. 1 as dotted curves. The values of the renormalization factor N_r are different from unity and are different for the different energies. This is in line with the results obtained in the previous studies including the one of Farid *et al.* [6].

In the second step of the analysis with the MGD distribution, the α-N interaction potential is added to the α-α attractive potential (still keeping the repulsive α-α potential depth, $V_R = 0.0$) to derive the folded α-nucleus potential. The values of $\rho^{\rm G}_{0\alpha}$, $\rho^{\rm G}_{0N}$ and β_N (the density parameters of the unclustered nucleons), and the parameters of the imaginary potential W_0 and R_W have been adjusted to obtain the best overall fits to the data at all the energies. The values of the energy-independent parameters are now $\rho^{\rm G}_{0\alpha} = 0.0248\,{\rm fm}^{-3}$, $\rho^{\rm G}_{0N} = 0.254\,{\rm fm}^{-3}$, $\beta_\alpha = 0.292\,{\rm fm}^{-2}$, $\beta_N = 1.2\,{\rm fm}^{-2}$, $w_{\rm G} = 0.467\,{\rm fm}^{-2}$. These values yield $4A_\alpha = 11.9$, $A_N = 1.7$ and $A_T = 13.6$ to the normalization integrals in (15) and lead to the renormalization factor as $N_r = 0.85$ in (16). The volume integral for the real part is now $J_R/(4A) = 358.2\,{\rm MeVfm}^3$. Three important points to be noted are:
i) The β_N value has to be substantially increased (the radius of density distribution for the unclustered nucleons decreased) to $\beta_N = 1.2\,{\rm fm}^{-2}$ to improve the fits.
ii) The renormalization factor $N_r = 0.82$, although different from unity, does not change with the incident energy.
iii) The total χ^2 is greatly reduced to $\chi^2_T = 19433$ from the previous value 50211, obtained without the inclusion of the α-N interaction in the folded potential.
The W_0 and χ^2 values at the different energies are given in table 2. The fits are shown in fig. 1 in dashed curves.

In the final step of the analysis with the MGD distribution, the repulsive part of the α-α potential has been turned on. The depth V_R and its range μ_R parameters have been searched upon for the best overall fits. The values of $\rho^{\rm G}_{0\alpha}$, $\rho^{\rm G}_{0N}$ and W_0 have been tuned to achieve further improvements in the fits. The final values of the energy-independent parameters are $\rho^{\rm G}_{0\alpha} = 0.0292\,{\rm fm}^{-3}$, $\rho^{\rm G}_{0N} = 0.298\,{\rm fm}^{-3}$, $\beta_\alpha = 0.292\,{\rm fm}^{-2}$, $\beta_N = 1.2\,{\rm fm}^{-2}$, $w_{\rm G} = 0.467\,{\rm fm}^{-2}$, $R_W = 3.45$ fm and $\mu_R = 0.5\,{\rm fm}^{-1}$. The parameters of the density distribution lead to $4A_\alpha = 14.0$, $A_N = 2.0$ and $A_T = 16.0$.

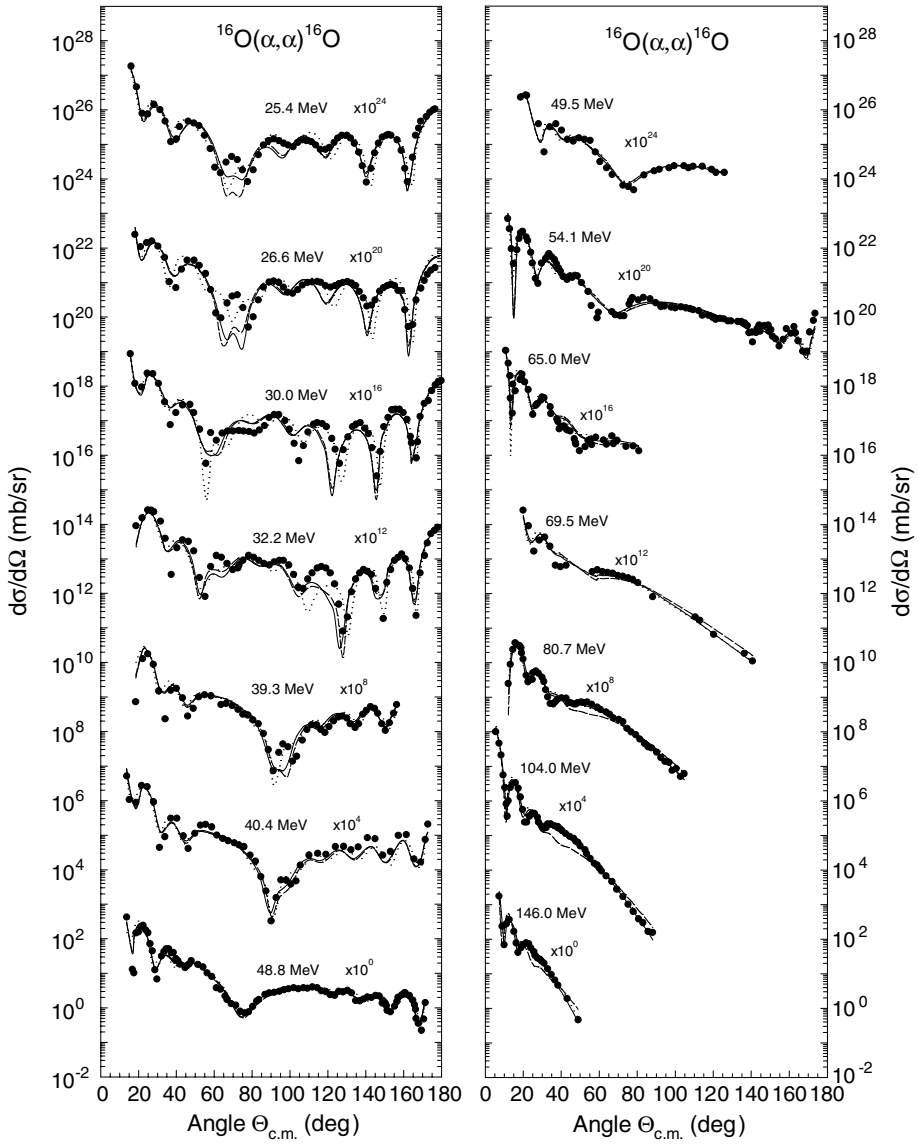

Fig. 1. Differential cross-sections for α+^{16}O elastic scattering at different energies are compared to the predictions from folded potentials using the modified Gaussian density distribution. The solid curves are calculations with the total contributions from the α-α (attractive and repulsive) and α-N potentials, the dashed curves, with the contributions from the α-α attractive (but without repulsive) and α-N potentials, and the dotted curves, with only the attractive part of the α-α potential. The data are from [10,12,17–20].

The important points that emerge from this step are:
i) The addition of the repulsive α-α interaction improves the fits to the data, particularly at the higher energies. The total χ^2 value reduces to $\chi^2_T = 17085$.
ii) The number of nucleons needed for the best fits is $A_T = 16.0$, $4A_\alpha = 14.0$ existing in α-like clusters and the remaining $A_N = 2.0$ in an unclustered form.
iii) The renormalization factor N_r is exactly unity and remains so at all incident energies.
The values of the energy-dependent parameters W_0, V_R, and the volume integrals $J_R/(4A)$ and $J_I/(4A)$ are listed in table 2. The fits are displayed in fig. 1 in solid curves. The root-mean-square (rms) radius for ^{16}O, deduced from the parameters of the density distribution, is obtained as $\langle r^2\rangle^{\frac{1}{2}} = 2.60$ fm, which compares well with the value ~ 2.7 fm quoted in Buck *et al.* [29] and de Vries *et al.* [30], but disagrees with the value 3.4 fm that can be obtained for ^{16}O from eq. (16) of Farid *et al.* [6].

3.2 Analysis using the 3-point Fermi distribution

In the second phase, the analysis has been repeated using the 3-point Fermi density (3FD) distribution for the α-like clusters and unclustered nucleons. The starting parameters $w_{\rm F} = -0.051$, $c_\alpha = c_N = 2.608$ fm and $a_\alpha = a_N = 0.513$ fm have been taken from de Vries *et al.* [30]. The first step of the analysis has been performed using only the α-α attractive potential. The data favor a

Table 2. Energy-dependent parameters in the second (using the α-α attractive and α-N potentials) and final (using the full α-α potential including the repulsive part and α-N potential) steps of the analysis with the modified Gaussian density-distribution. E_α, V_R and W_0 are in MeV, and $J_R/(4A)$ and $J_I/(4A)$ are in MeVfm^3.

	Second step with Gaussian distribution				Final step with Gaussian distribution				
E_α	W_0	χ^2	$J_R/(4A)$	$J_I/(4A)$	V_R	W_0	χ^2	$J_R/(4A)$	$J_I/(4A)$
25.4	8.5	620	358.2	28.0	27.2	8.5	692	360.8	28.0
26.6	10.3	1415		34.0	28.0	10.4	1136	359.0	34.3
30.0	10.6	3110		35.0	31.6	10.5	3281	351.0	34.6
32.2	13.0	2857		42.9	31.7	13.2	2791	350.8	43.6
39.3	16.8	2593		55.4	31.8	16.4	2580	350.6	54.1
40.4	16.9	551		55.8	31.9	16.5	678	350.5	55.4
48.8	18.2	4228		60.0	32.0	17.5	3489	350.1	57.7
49.5	21.0	482		69.3	32.1	21.0	466	349.9	69.3
54.1	22.5	891		74.2	33.0	22.0	719	347.9	72.6
65.0	29.4	1005		97.0	37.4	27.9	724	338.9	92.0
69.5	29.5	307		97.3	37.5	28.0	202	337.9	92.4
80.7	34.0	381		112.2	47.0	28.9	147	316.7	95.4
104.0	42.0	635		138.6	61.0	29.7	102	285.5	98.0
146.0	48.0	358		158.4	78.0	30.2	81.3	247.6	99.6

Table 3. Energy-dependent parameters in the first (using only the attractive part of α-α potential), second (using the α-α attractive and α-N potentials) and final (using the full α-α interaction including the repulsive part and α-N potential) steps of the analysis with the 3-point Fermi density distribution. E_α, V_R and W_0 are in MeV, and $J_R/(4A)$ and $J_I/(4A)$ are in MeVfm^3.

	First step		Second step		Final step				
E_α	W_0	χ^2	W_0	χ^2	V_R	W_0	χ^2	$J_R/(4A)$	$J_I/(4A)$
25.4	8.5	1051	8.5	808	32.8	8.6	739	348.4	27.2
26.6	10.2	1295	10.7	1228	32.9	10.5	1322	348.2	33.2
30.0	10.5	2046	11.0	2819	37.0	11.0	2962	339.0	34.7
32.2	13.0	1478	13.2	2296	37.1	13.2	3357	338.8	41.7
39.3	17.2	1918	17.2	915	37.2	16.8	1074	338.6	53.1
40.4	17.3	484	17.3	648	37.3	16.9	787	338.4	53.4
48.8	19.2	3456	18.2	2082	37.4	17.9	1203	338.2	56.5
49.5	22.0	452	21.0	278	37.5	21.3	232	337.9	67.3
54.1	24.0	970	23.5	807	39.0	22.5	578	334.6	71.1
65.0	32.9	830	31.0	732	45.0	28.5	494	321.3	90.0
69.5	33.0	2786	31.1	267	45.1	28.6	95.6	321.1	90.3
80.7	37.0	436	33.5	411	53.0	29.5	120	303.5	93.2
104.0	45.0	891	43.0	803	65.0	30.2	69.4	276.8	95.4
146.0	52.0	336	50.0	258	76.0	31.8	84.4	250.2	100.4

reduced value of diffuseness to $a_\alpha = 0.430$ fm. Satisfactory fits to the data can be achieved with the parameters $\rho^{\rm F}_{0\alpha} = 0.0433\,{\rm fm}^{-3}$, $c_\alpha = 2.608$ fm, $a_\alpha = 0.430$ fm, $w_{\rm F} = -0.051$ and $R_W = 3.35$ fm. The fits to data using the values of the energy-dependent parameter W_0 and χ^2-values are shown in table 3, and displayed in fig. 2 as dotted curves. The total χ^2 value is $\chi^2_T = 15922$, which is even lower than the best figure achieved with the MGD distribution. The parameters of the density distribution yields $A_T = 4A_\alpha = 15.5$, which leads to the energy-independent renormalization factor $N_r = 0.969$. Thus, with the 3FD distribution one can generate from only the attractive part of α-α potential a folded potential, which does not need renormalization at different energies. The energy independence of the renormalization factor has not been achieved using the MGD distribution in the first phase of our analysis.

In the second step, the effect of addition of the α-N interaction without the inclusion of the repulsive potential to the α-α attractive potential is examined. R_W, c_α, $w_{\rm F}$, a_α and a_N are kept unchanged, but the radius c_N of the density distribution for the unclustered nucleon has to be reduced to obtain satisfactory fits to the data. The values of the best-fit energy-independent parameters are $\rho^{\rm F}_{0\alpha} = 0.0363\,{\rm fm}^{-3}$, $\rho^{\rm F}_{0N} = 0.0820\,{\rm fm}^{-3}$, $c_\alpha = 2.608$ fm, $c_N = 1.1$ fm, $a_\alpha = a_N = 0.430$, $w_{\rm F} = -0.051$ and $R_W = 3.40$ fm. The values of W_0 and the χ^2-values for different energies are noted in table 3. The fits are shown

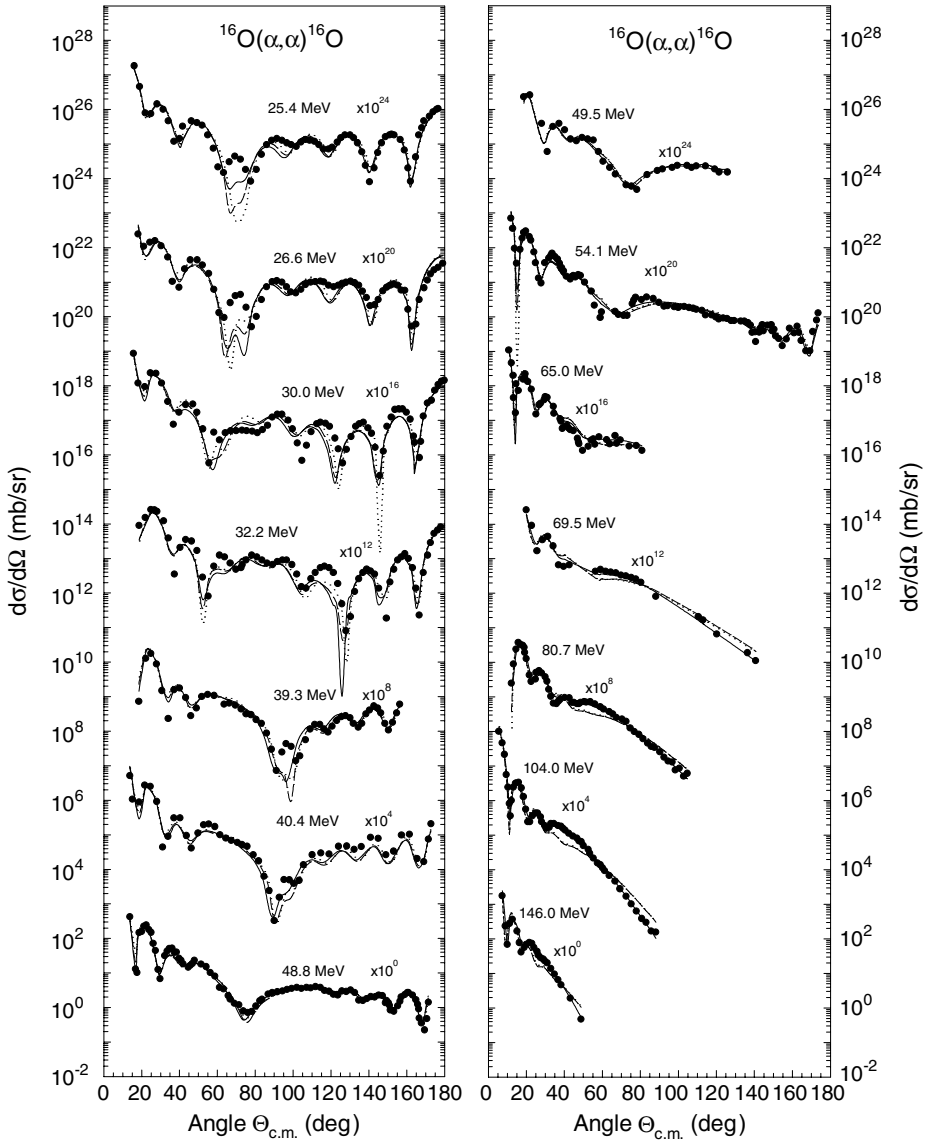

Fig. 2. Same as in fig. 1, but for the 3-point Fermi density distribution.

in fig. 2 as broken curves. The total χ^2 value reduces to $\chi^2_T = 14351$, indicating that the fits are improved, in particular, to the data of lower incident energies, with the inclusion of the α-N potential. The normalization integrals are now $4A_\alpha = 13.0$, $A_N = 1.0$ and $A_T = 14.0$. This corresponds to the value $N_r = 0.875$ for the renormalization factor, which is again energy independent.

In the final step of the analysis with the 3FD distribution, the repulsive part of α-α potential is added to the α-α attractive and α-N interaction potentials. If the parameter values $c_\alpha = 2.608$ fm, $a_\alpha = a_N = 0.430$ fm and $R_W = 3.40$ fm are left unchanged, the best overall fits to the data over the entire 25.4–146.0 MeV incident-energy range can be realized with the following conditions:
i) The central densities $\rho^{\rm F}_{0\alpha} = 0.0391\,{\rm fm}^{-3}$ and $\rho^{\rm F}_{0N} = 0.164\,{\rm fm}^{-3}$ are needed.
ii) The radius of the unclustered nucleonic density distribution, has to be $c_N = 1.1$ fm, again much less than that for the α-like distribution $c_\alpha = 2.608$ fm, as observed in the second step of the analysis.
iii) The range parameter of the repulsive potential is $\mu_R = 0.5\,{\rm fm}^{-1}$.
The values of the energy-dependent parameters V_R and W_0, the volume integrals $J_R/(4A)$ and $J_I/(4A)$, and χ^2 values are listed in table 3. The deduced values of the normalization integrals in (15) are (again, as obtained in the final analysis with the MGD distribution) $4A_\alpha = 14.0$, $A_N = 2.0$ and $A_T = 16.0$, which gives the renormalization factor as $N_r = 1.0$ and energy independent. The fits are shown in fig. 2 in solid curves. The total χ^2 value is further reduced to $\chi^2_T = 13118$ with the inclusion of the repulsive potential, from 14351 obtained in the second phase without the repulsive potential. The effect of the repulsive potential is particularly tangible in fits to the data of higher energies. The overall fits, obtained with the 3FD distribution, are better than those generated by the folded

Table 4. Energy-independent parameters including those relating density distributions.

Parameter	Modified Gaussian distribution			Parameter	3-point Fermi distribution		
	First step	Second step	Final step		First step	Second step	Final step
V_A (MeV)	122.62	122.62	122.62	V_A (MeV)	122.62	122.62	122.62
μ_A (fm)	0.469	0.469	0.469	μ_A (fm)	0.469	0.469	0.469
μ_R (fm)	0.50	0.50	0.50	μ_R (fm)	0.50	0.50	0.50
V_0 (MeV)	47.3	47.3	47.3	V_0 (MeV)	47.3	47.3	47.3
K (fm^{-1})	0.435	0.435	0.435	K (fm^{-1})	0.435	0.435	0.435
R_W (fm)	3.55	3.45	3.45	R_W (fm)	3.35	3.40	3.40
$\rho^{\rm G}_{0\alpha}$ (fm^{-3})	*	0.0248	0.0292	$\rho^{\rm F}_{0\alpha}$ (fm^{-3})	0.0433	0.0363	0.0391
$\rho^{\rm G}_{0N}$ (fm^{-3})	0.0	0.2540	0.2980	$\rho^{\rm F}_{0N}$ (fm^{-3})	0.0	0.0820	0.1640
β_α (fm^{-2})	0.292	0.292	0.292	c_α (fm)	2.608	2.608	2.608
β_N (fm^{-2})	–	1.2	1.2	c_N (fm)	–	1.1	1.1
–	–	–	–	a_α (fm)	0.430	0.430	0.430
–	–	–	–	a_N (fm)	0.430	0.430	0.430
$w_{\rm G}$ (fm^{-2})	0.467	0.467	0.467	$w_{\rm F}$	-0.051	-0.051	-0.051
$4A_\alpha$	*	11.9	14.0	$4A_\alpha$	15.5	13.0	14.0
A_N	0.0	1.70	2.00	A_N	0.0	1.0	2.0
A_T	*	13.6	16.0	A_T	15.5	14.0	16.0
N_r	*	0.650	1.0	N_r	0.969	0.875	1.0
χ^2_T	50211	19433	17085	χ^2_T	15992	14351	13118

* The values are energy dependent and given in table 1.

potential from the MGD distribution. The rms radius for the density distributions is found as $\langle r^2\rangle^{\frac{1}{2}} = 2.52$ fm.

The values of the energy-independent parameters used in three steps of the analysis with MGD and 3FD distributions, and the derived results are summarized in table 4.

4 Discussion and conclusions

The present work gives a simple prescription of a single-folded potential, which provides a satisfactory account of the data of the α-elastic scattering on ^{16}O over a broad range of incident energies, namely, 25.4–146.0 MeV. The derived potential, in the present work, does not need any renormalization for a satisfactory description of the data over the entire energy range including six energy points at 25.4, 26.6, 30.0, 39.3, 49.5 and 69.5 MeV, not considered in Farid *et al.* [6]. The number of energy-dependent parameters in the present folded potential is just two, namely, the depth parameters V_R and W_0, while that in the work of Farid *et al.* [6] involves four energy-dependent parameters, *e.g.*, the renormalization factor, and three parameters of imaginary potentials. The inclusion of the α-N interaction to the α-α attractive potential, *i.e.* simultaneous consideration of density distribution of α-like clusters and unclustered nucleons in ^{16}O, removes the energy dependence of the renormalization factor N_r, as in table 1, needed to fit the data with only the α-α attractive potential for the case of the MGD distribution, and improves the χ^2_T-value for the fits to the data (table 4) for both the density distributions considered in the present work. The slow energy dependence of the real part of the α-nucleus interaction is contained in the repulsive part of the α-α interaction. The addition of repulsive part decreases the χ^2_T values further for the overall fits, particularly at the larger incident energies and its inclusion coupled with the consideration of unclustered nucleons, yields the renormalization factor to exactly $N_r = 1.0$ (table 4) for both the density distributions considered herein. The ℓ-independent repulsive part, used in the present work, is found to work well and this aspect of the potential gives it a more usable form. The addition of the repulsive part conforms to the Pauli principle. The results of the present analysis suggest that the repulsive part is expected to show up prominently in the α-α elastic scattering at higher energies as well.

The inclusion of the supplementary folding potential arising from the unclustered nucleons in the target nucleus along with the α-α repulsive potential, in the present work, solves the long-standing problem with renormalization of the folded potential. Both the MGD and 3FD distributions give identical results, which are as follows:
i) Both the density distributions generate similar volume integrals for the real and imaginary parts of the α-^{16}O interaction potential. $J_R/(4A)$ varies from 360.8 MeVfm^3 at 25.4 MeV to 247.6 MeVfm^3 (table 2) for the MGD distribution, while the 3FD distribution gives the corresponding values from 351.3 to 250.2 MeVfm^3 (table 3) in the same range of energies. $J_I/(4A)$ varies from 28.0 to 99.6 MeVfm^3 for the former distribution and 27.2 to 100.4 MeVfm^3 for the latter one.

ii) Both the distributions generate the same number of nucleons A_T (table 4) forming the α-like clusters with $4A_\alpha = 14.0$ nucleons in them, and $A_N = 2.0$ unclustered nucleons in ^{16}O in the time-averaged picture. All the nucleons in the target participate in generating the folding potential.
iii) The deduced values of the rms radius from the Gaussian and Fermi distributions are, respectively, $\langle r^2\rangle^{\frac{1}{2}} = 2.60$ and 2.52 fm, which compare well with the quoted value of ~ 2.7 fm in the literature [29,30]. The latter distribution, however, generates better overall fits to the data.
iv) The calculations with both the density distributions suggest that the radius of the unclustered nucleonic distribution is much less than that for the α-like clusters. This is in conformity with the calculations of Brink and Castro [2], Mueller and Clark [33] and Roepke [34] that the α-particle formation is energetically favored in the region of nuclear surface.
The quality of fits to the angular distribution data at different incident energies suggests that the approximations made in generating the folding potential are appropriate. It is remarkable that the use of the observed density distribution in [30], which is a manifestation of the nucleonic and other cluster-like configurations, can successfully account for the α-^{16}O elastic scattering over a wide range of energies without any need to renormalize the folded potential, generated from the distribution with a simple prescription suggested herein. The folding model, used in the present work, is expected to work for any non-α cluster nucleus and demands further attention. It remains to be seen whether the cluster formalism can describe a whole range of phenomena in a unified way, as observed by Hodgson [35].

This work is partly supported by the grant INT-0209584 of the U.S. National Science Foundation and a grant from the Ministry of Science and Technology, Government of Bangladesh, which are thankfully acknowledged. The authors are thankful to Dr. Peter E. Hodgson of the Nuclear Physics Laboratory, University of Oxford, for encouraging and helping the work by supplying many preprints and reprints of published articles to them in Rajshahi. One of the authors (AKB) is thankful to the American Institute for Bangladesh Studies for supporting the visit to the USA in 2002 to complete the work.

References

1. J.A. Wheeler, Phys. Rev. **52**, 1083 (1937).
2. D. Brink, J.J. Castro, Nucl. Phys. A **216**, 109 (1973).
3. Li Qing-Run, Yang Yong-Xu, Nucl. Phys. A **561**, 181 (1993).
4. Y.-X. Yang, Q.-R. Li, Europhys. Lett. **21**, 657 (1993).
5. M. El-Azab Farid, J. Phys. G **16**, 461 (1990).
6. M. El-Azab Farid, Z.M.M. Mahmoud, G.S. Hassan, Phys. Rev. C **64**, 014310 (2001).
7. P.P. Singh, P. Schwandt, G.C. Yang, Phys. Lett. B **59**, 113 (1975).
8. R. Neu, H. Abele, P.D. Eversheim, F. Hinterberger , H. Oberhummer, H. Jäntach, Ch. Striebel, G. Staudt, M. Walz, J. Phys. Soc. Jpn. Suppl. **58**, 574 (1989).
9. A.M. Kobos, B.A. Brown, R. Lindsay, G.R. Satchler, Nucl. Phys. A **425**, 205 (1984).
10. H. Abele, G. Staudt, Phys. Rev. C **47**, 742 (1993).
11. U. Atzrott, P. Mohr, H. Abele, C. Hillenmayer, G. Staudt, Phys. Rev. C **53**, 1336 (1996).
12. H. Abele, H.J. Hauser, A. Körber, W. Leitner, R. Neu, H. Plappert, T. Rohwer, G. Staudt, M. Straßer, S. Welte, M. Walz, P.D. Eversheim, F. Hinterberger, Z. Phys. A **326**, 373 (1987).
13. G. Bertsch, J. Borysowicz, H. McManus, W.G. Love, Nucl. Phys. A **284**, 399 (1977).
14. Dao T. Khoa, G.R. Satchler, W. von Oertzen, Phys. Rev. C **56**, 954 (1997).
15. Dao T. Khoa, Phys. Rev. C **63**, 034007 (2001).
16. S.A.E. Khallaf, A.M.A. Amry, S.R. Mokhtar, Phys. Rev. C **56**, 2093 (1997).
17. A.A. Cowley, G. Heymann, Nucl. Phys. A **146**, 465 (1970).
18. F. Michel, J. Albinski, P. Belery, Th. Delbar, Gh. Grégoire, B. Tasiaux, G. Reidemeister, Phys. Rev. C **28**, 1904 (1983).
19. G. Hauser, R. Löhken, H. Rebel, G. Schatz, G.W. Schweiner, J. Specht, Nucl. Phys. A **128**, 81 (1969).
20. K.T. Knöpfle, G.J. Wagner, H. Breuer, M. Rogge, C. Mayer-Bricke, Phys. Rev. Lett. **35**, 779 (1975).
21. B. Block, J.W. Clark, M.D. High, R. Malmin, F.B. Malik, Ann. Phys. (N.Y.) **62**, 464 (1971).
22. H. Feshbach, Ann. Phys. (N.Y.) **5**, 357 (1958).
23. H. Feshbach, Ann. Phys. (N.Y.) **19**, 287 (1962).
24. N. Austern, Ann. Phys. (N.Y.) **45**, 113 (1967).
25. B. Buck, H. Friedrich, C. Wheatley, Nucl. Phys. A **275**, 246 (1977).
26. S. Ali, A.R. Bodmer, Nucl. Phys. **80**, 99 (1966).
27. S. Ali, A.A.Z. Ahmad, N. Ferdous, Rev. Mod. Phys. **57**, 923 (1985).
28. S. Sack, L.C. Biedenharn, G. Breit, Phys. Rev. **93**, 321 (1954).
29. B. Buck, H. Friedrich, C. Wheatley, Phys. Rev. C **11**, 1803 (1975).
30. H. de Vries, C.W. de Jager, C. de Vries, At. Data Nucl. Data Tables **36**, 495 (1987).
31. O. Bersillon, SCAT2 code, NEA 0289, 1988.
32. F. James, M. Roos, Comput. Phys. Commun. **10**, 343 (1975).
33. G.P. Mueller, J.W. Clark, Nucl. Phys. A **155**, 561 (1970).
34. G. Roepke, Cond. Matter Theories **16**, 468 (2001).
35. P.E. Hodgson, Contemp. Phys. **31**, 99 (1990).